

ORIGINAL PAPER

Preliminary Safety Analysis on Depressurization Accident without Scram of a Molten Salt Reactor

Nobuhide SUZUKI[†] and Yoichiro SHIMAZU*

Graduate School of Engineering, Hokkaido University, Kita 13, Nishi 8, Kita-ku, Sapporo 060-8628, Japan

(Received April 6, 2005 and accepted in revised form March 10, 2006)

The Molten Salt Reactor (MSR) concept has recently been considered as one of the candidates for the generation IV nuclear power systems. MSRs have many advantages such as improved safety, proliferation resistance, resource sustainability and waste reduction. But MSR developmental activities have lagged and there are few data available to support detailed analyses. However, the authors believe that additional investigations are merited for future study. From this point of view, the authors have analyzed the depressurization accident of the MSR “Fuji-12” using a newly developed MSR transient analysis code. In Fuji-12, a small amount of helium gas bubbles are circulated in the primary loop for stripping out gaseous fission products. A depressurization of the primary system would cause these bubbles to expand, resulting in a positive reactivity insertion. We have attempted to determine the severity of such an accident. Although the analysis is still preliminary and the assumptions are crude, it can be expected that the depressurization would not result in a severe accident in Fuji-12.

KEYWORDS: *safety analysis, depressurization accident, molten salt reactor (MSR), transient analysis, Fuji-12, void reactivity coefficient*

I. Introduction

Molten Salt Reactors (MSRs) have a long history with the first design studies beginning in the 1950’s at the Oak Ridge National Laboratory (ORNL). One of the results from these early and extensive studies was reported in ORNL-4541,¹⁾ entitled “Conceptual Design of a Single Fluid Molten Salt Breeder Reactor.” However the developmental efforts have slowed considerably, except for some small scale efforts, mostly in Russia, France, Japan and a few other places. Recently, a conceptual design of a small MSR, name Fuji-12^{2,3)} has been proposed. Fuji-12 operates with the same fuel salt as the Molten Salt Breeder Reactor (MSBR) designed by ORNL. But it differs from the ORNL design in several ways, such as no on-site chemical processing plant and a low rated power. The authors are interested in the MSR concept due to its high potential in the areas of safety, proliferation resistance, resource sustainability and waste reduction, all necessary requirements for the generation IV nuclear power systems as stated in “A Technology Roadmap for Generation IV Nuclear Energy Systems,” GIF-002-00, Dec. (2002) by U.S. DOE. Therefore the MSR concept has been selected as one of the more promising candidates for future consideration.

In MSRs some gaseous fission products such as xenon and krypton are stripped out by helium gas bubbles circulated in the primary fuel salt. Although the operating fuel salt temperature is lower than the boiling temperature at atmospheric pressure, the primary salt pressure is higher because of the circulation. Thus when the primary loop integrity is lost,

the pressure could be reduced and the bubbles would expand. Due to the low pressure of the fuel salt in the primary loop, the discharge speed of the fuel salt is expected to be small. However, since the void reactivity coefficient of MSRs is positive, the incident could result in a reactivity insertion accident. It is sometimes pointed out that this characteristic of MSRs is fatal. With this in mind, we investigated the safety of Fuji-12 assuming a depressurization accident using the MSBR system parameters. The analysis is still preliminary and the assumptions are relatively crude because the developmental activities on MSR have been sparse. Since there are few theoretical or experimental data available for detailed analyses, we used simple assumptions and data previously published. However, such a preliminary study can give us information about necessary and indispensable data and experiments that can be applied in future accident analyses. Moreover, it might be helpful to know the worst case transient in order to plan counter measures against such an accident. We therefore assumed that no scram would take place. We do not claim that this accident represents the only possible accident in MSRs. We will continue to investigate the safety of MSRs in the near future.

II. Description of Fuji-12 Design

A schematic design of the reactor core is shown in Fig. 1.⁴⁾ The reactor is a graphite moderated thermal reactor composed of the core and the reflector, consisting of many hexagonal prismatic elements made of high density graphite. The elements are surrounded by a neutron absorber made of boron carbide, and all these structures are contained in the reactor vessel made of modified Hastelloy-N. The fuel salt is made of LiF-BeF₂-ThF₄-UF₄. It flows into the reactor through the lower entrances at 840 K, flows upwards through passages in the graphite elements where the temperature in-

*Corresponding author, E-mail: shimazu@eng.hokudai.ac.jp

[†]Present address: Mitsubishi Heavy Industries, Ltd., 1-1, Wadasaki-cho 1-chome, Hyogo-ku, Kobe 652-8585, Japan

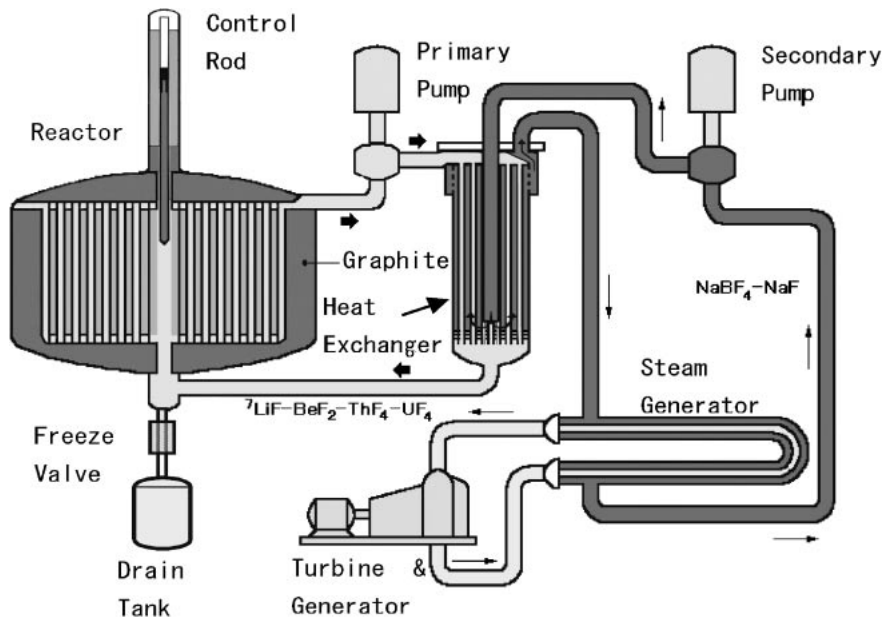


Fig. 1 Schematic view of Fuji-12

creases due to nuclear fission reactions and then flows out of the reactor through the upper outlets at 980 K. The reactor can operate for an extended period without continuous fuel reprocessing and without graphite replacement in the core. The main design parameters are listed in **Table 1**. These parameters are typical values. The characteristics of MSR are relatively independent of core lifetime. The specifications of the heat exchanger and the primary loop are also listed in Table 1. These parameters were evaluated by analogy with the design values of the MSBR.

III. Description of the Primary Loop Simulator

The authors developed a new simulator in r-z geometry for the MSR transient analysis. As the MSR has a completely radial symmetry and the fuel characteristics in the core are almost homogeneous, the r-z geometry can be applied to a wide range of core configurations. It is based on a two-group neutron diffusion model with both reactor kinetics calculation and thermal analysis of the primary loop. The number of calculation meshes is 25 in the radial direction and 52 in the axial direction for reactor and reflector with a mesh size of 10 cm. There is a fuel plenum zone at the top and bottom of the reactor that is represented by a single mesh with a width of 2.5 cm. The outer loop is divided into 140 equal volume nodes.

The reactor kinetics is solved using the stiffness confinement method (SCM) with a calculation time interval of 0.01 s and includes the plant dynamics.⁵⁾ Six-group delayed neutrons are considered and they are calculated in each mesh. The circulation of the fuel salt in the reactor and the loop is also taken into account.

The thermal analysis utilizes a typical heat transfer model. The graphite core blocks have a central fuel passage with a diameter of about 10 cm. The fuel salt flows upward within

Table 1 Principal design parameters of Fuji-12

Thermal capacity	350 MWth
Net electric generation	150 MWe
Thermal efficiency	43%
Number of coolant loops	2
Core	
Radius/Height	2.0/4.0 m
Graphite fraction	70 vol%
Reflector	
Thickness rad./Axi.	0.5/0.6 m
Graphite fraction	99 vol%
Average power density	7.0 kWth/l
Specifications of heat exchanger	
Thermal capacity	350 MW
Tube length	6.8 m
Total heat transfer area	760 m ²
Fuel salt volume	1.19 m ³
Fuel salt speed in heat exchanger	3.14 m/s
Fuel salt temperatures Inlet/Outlet	980 K/840 K
Coolant volume	7.25 m ³
Coolant speed	1.22 m/s
Coolant temperature (Inlet/Outlet)	765 K/670 K
Total length of primary loop	7.2 m
Fuel salt speed in primary loop	1.2 m/s
Fuel Salt	
Composition	
LiF	Balance
BeF ₂	16.0 mol%
ThF ₄	12.0 mol%
UF ₄	0.22 mol%
Volume in Reactor	15.7 m ³
Total Volume	20.2 m ³
Flow Rate	0.55 m ³ /s
Temperature Inlet/Outlet	840 K/980 K

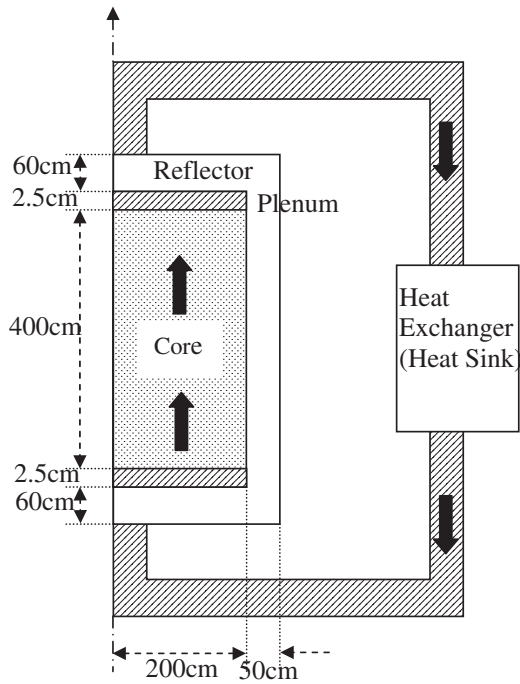


Fig. 2 Model for the calculation

this closed channel. Thus the flow analysis uses a simple axial flow model. It assumes that some portion of heat from the fuel is transferred to the graphite moderator. The temperature distributions of fuel salt and graphite blocks in the core are used to calculate the reactivity feedback for the neutronic calculation until the entire core calculation converges. Then the heat generated by fission is transferred by the heated molten fuel salt to the primary heat exchanger and the cooled fuel salt is returned back to the reactor. The radial fuel flow distribution is assumed to be such that the temperature rise in the reactor is homogeneous. The heat removal in the primary heat exchanger is assumed to be constant during the transient. The basis of this assumption is discussed later in Sec. IV-5.

The model for the calculation is shown in Fig. 2. The actual reactor geometry is such that the core radius is 200 cm and the height is 400 cm. The thicknesses of the radial and axial reflector are 50 cm and 60 cm, respectively, and the widths of the top and bottom core plenums of the core are 2.5 cm each.

The nuclear constants are calculated by SRAC95 developed by Japan Atomic Energy Research Institute (JAERI).⁶⁾ First of all, cell calculations for various graphite blocks with respective fuel passages are calculated using the SRAC-PIJ module. The nuclear data file is JENDL-3.2 and the number of energy group is 107. Based on this calculation, two group nuclear constants are obtained for the core analyses by the CITATION module. Fuel composition is assumed to be identical to those reported in Ref. 3). In MSR, no burnup distribution exists and the core characteristics are not so time dependent. The kinetic parameters are obtained through the CITATION calculation and are listed in Table 2.

Table 2 Delayed neutron constants

i (group)	β_i	λ_i
1	2.34171×10^{-4}	1.25964×10^{-2}
2	8.18020×10^{-4}	3.34000×10^{-2}
3	6.92913×10^{-4}	1.30706×10^{-1}
4	7.97878×10^{-4}	3.03222×10^{-1}
5	1.57349×10^{-4}	1.23167×10^{-0}
6	9.61766×10^{-5}	3.13831×10^{-0}

IV. Depressurization Accident Analysis

1. Depressurization Accident

The MSR is equipped with a helium gas bubble generator that produces bubbles with a diameter of 0.05 cm. These are circulated in the primary loop in order to strip out gaseous fission products. The average void fraction of helium is expected to be about 0.2% in the fuel salt in order to reduce the Xe poisoning fraction to less than 0.5%.¹⁾ The MSR operating pressure is not atmospheric even though the fuel salt vapor pressure is quite low. Some pressure must be applied for the circulation of the fuel salt. The average pressure in the reactor was evaluated as 0.46 MPa for the MSBR. Under such operating conditions, when a break occurs in one of the two primary loops, the fuel salt is lost and the volume will then be filled by the expansion of the helium bubbles. The system pressure transients will depend on the location of the break. They can be roughly classified into the following three cases.

Case 1: Break between the fuel salt pump exit and the heat exchanger

In this case the break occurs where the fuel salt pressure is the highest. The fuel flows out of the break due to the high pressure and the fuel flow will be lost. In order to avoid the loss of a large amount of fuel salt from the reactor vessel, we assume that this loop is isolated. Thus the salt flow of the reactor becomes half of the rated value. In other words, this is an accident of partial loss of fuel flow. In MSRs, the loss of fuel salt flow results in the loss of heat removal and also results in a small reactivity insertion due to the reduction of the loss of delayed neutrons from the core.

Case 2: Break near the reactor inlet

In this case the fuel will not only flow out due to the pressure difference between the inside and outside of the reactor loop but also by gravity. The fuel flows downward but the helium bubbles travel upward due to buoyancy. Thus the bubbles are separated from the fuel salt and the void fraction becomes zero in this region. It means that the expansion and the separation of the bubbles take place simultaneously in the core. When the separated bubbles reach the surface of the fuel salt, fuel salt is voided at the top region of the core. Therefore the fuel salt pump loses suction due to this voided region and fuel salt flow is lost. Thus it is assumed that the fuel salt flow is completely lost at the initiation of the accident. Negative reactivity is also added by the increased neutron leakage due to the decreased fuel volume. Finally, the fuel leak will cease when the negative inner pressure is balanced by the effect of the gravity.

Case 3: Break at the exit of the reactor

In this case the fuel salt will flow out due to the pressure difference until the inner pressure drops to atmospheric pressure. The full fuel salt flow could be maintained, however for this case we assumed that this loop was isolated.

2. Reactivity Evaluation

As described above, we must determine both the void fraction increase and the void reactivity coefficient for the evaluation of the reactivity insertion for the depressurization accident. The initial void fraction and the pressure are 0.2% and 0.46 MPa, respectively, according to the MSBR design. We believe that using these values for the accident analyses will include sufficiently conservative margins. The pressure drop and xenon concentration for Fuji-12 would be less than those for the MSBR because the average power density of Fuji-12 is one third of the MSBR.

The void reactivity coefficient is calculated by SRAC95 using the PIJ module for nuclear cell constants and the CITATION module for the reactor calculation in r-z cylindrical geometry. The result is shown in Table 3. The void reactivity coefficient, α_v , is positive and its value is $0.091\% \Delta k/k/\% \text{void}$.

3. Transient for Case 1—Evaluation of the loss of 50% fuel salt flow

The reactor transient was analyzed as follows. The thermal and hydraulic properties of fuel salt are assumed to stay constant as the void fraction of the circulated helium bubbles increases to around 1% at most. Therefore we calculated the reactor transient only by the reactor simulator and separate from the depressurization transient. The accident was assumed to occur when the reactor was operating at the rated

power. Also no scram action was assumed. That is, we analyzed the transient without scram. The fuel flow rate was reduced to 50% of the rated value at the initiation of the accident. In this case, no bubble expansion was assumed. The following sections would discuss the transient in the event that the bubbles expand.

With the initiation of this transient, the heat sink was partially lost and the system temperatures went up. At the same time, due to the loss of partial fuel flow, reactivity increased due to the reduction of the loss of delayed neutrons from the core. The transient of fuel salt and graphite temperatures are shown in Fig. 3. With these increases in temperature, negative reactivity was added and the power decreased and then stabilized at 50% of rated power. The power transient is shown in Fig. 4. As can be seen in this figure the effect of the temperature rise is larger than the delayed neutron effect. The temperatures are also stabilized at the initial condition with a small increase. The maximum outlet fuel temperature is 1,000 K.

In Fig. 4, the power transient behaves faster than the fuel temperature transient. This is because the temperatures in Fig. 4 are the average inlet and outlet temperatures. In Fig. 5 the transient of the maximum temperature of fuel salt in the core is compared with the outlet fuel temperature for a typical reactivity insertion with full fuel flow as an example. The maximum fuel temperature rises much faster and higher than the outlet fuel temperature. The rapid power decrease in the short time after the break is due to this rapid fuel temperature rise at the hot spot. It is common to all the transients shown below. The maximum temperatures occur in the center of the core near the exit, but there are no materials that could melt in this region, unlike conventional reactors. Thus the maximum temperature in this spot cannot be a limiting condition.

Table 3 Reactivity change due to void fraction change

Void fraction (%)	k_{eff}	ρ (% $\Delta k/k$)
0.3	1.019132	1.8773
1.5	1.020269	1.9866

4. Evaluation Model for the Depressurization Transient for Case 2

The transients for cases 2 and 3 were analyzed by a simple model that is based on the assumption that all the lost fuel volume is filled by the expansion of the helium originally

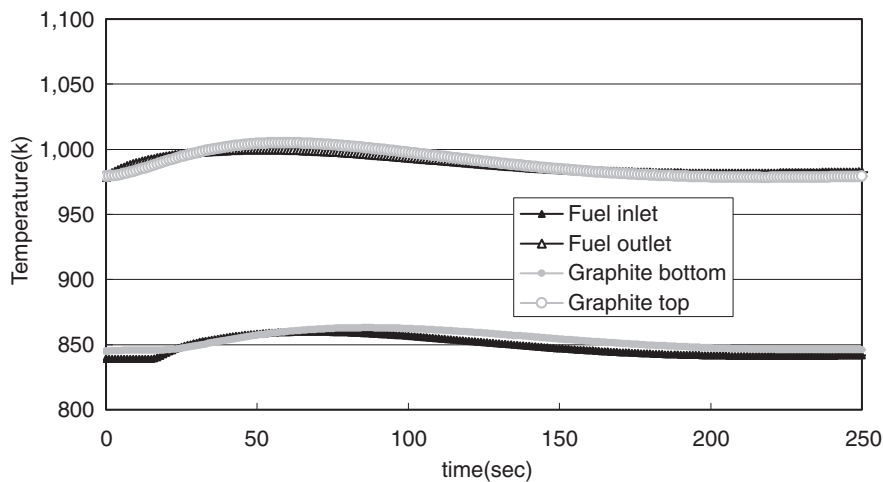


Fig. 3 Reactor transient for the loss of 50% flow of fuel salt: Temperatures

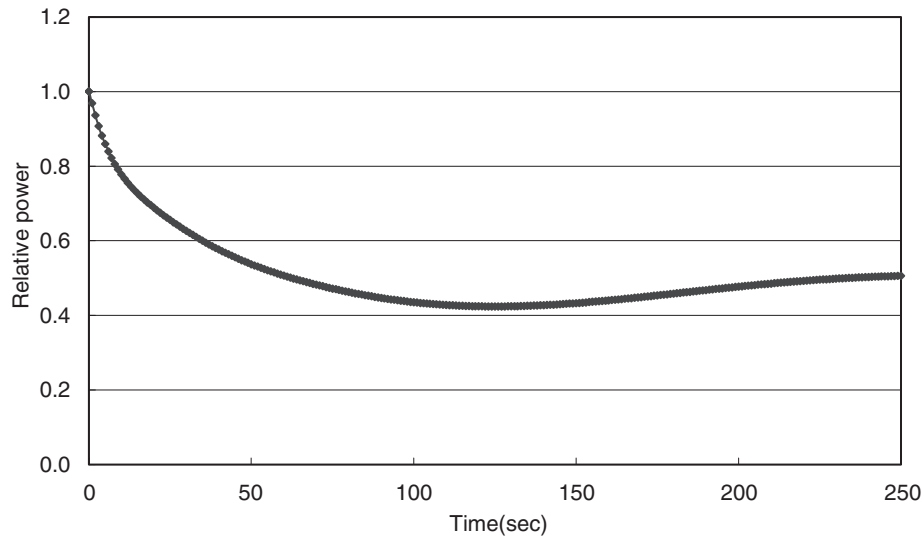


Fig. 4 Reactor transient for the loss of 50% flow of fuel salt: Relative power

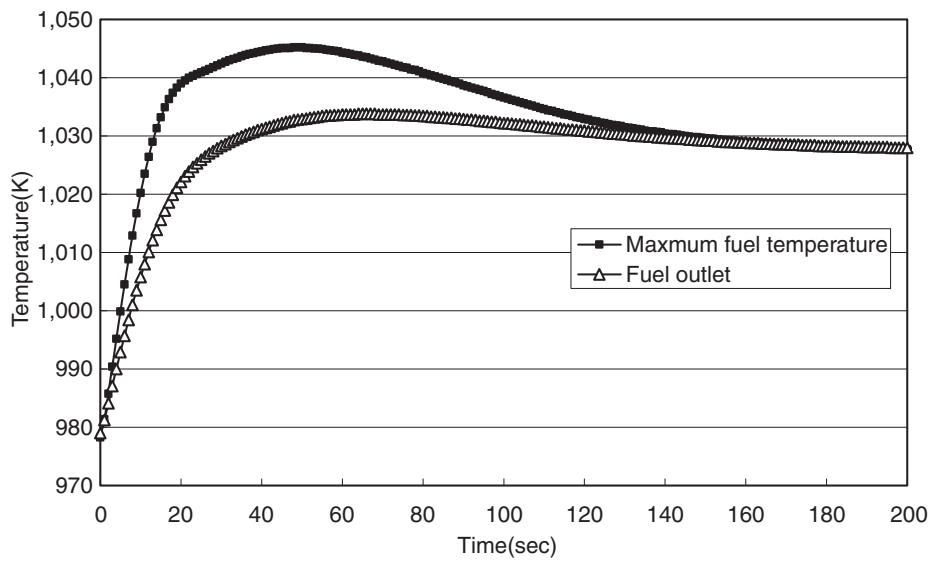


Fig. 5 Reactor transient after step reactivity addition: Maximum temperature in the core

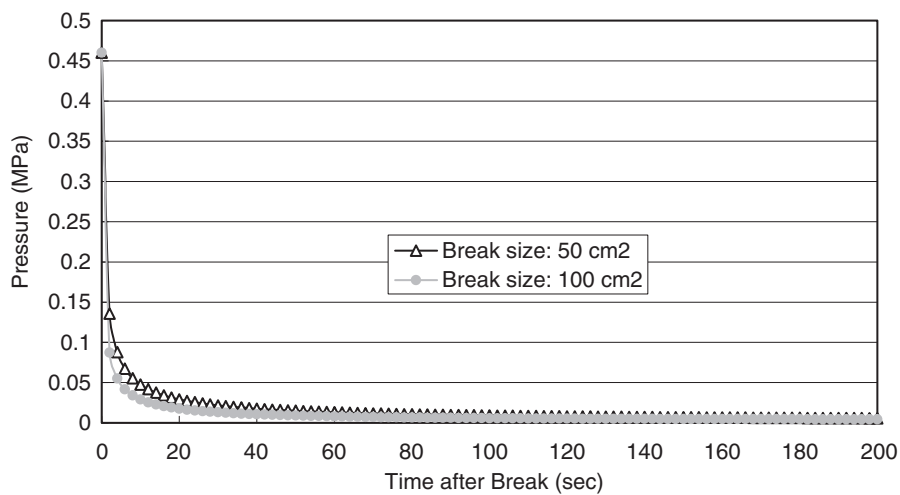


Fig. 6 Reactor pressure transient for the break near the reactor inlet

contained in the fuel salt. Since the fuel volume in the reactor is about 80% of the total system, the salt is assumed to be lumped in the reactor. Thus a simple discharge model is used as explained below. Note that this model is completely separated from the above mentioned primary loop simulation model. Isolation of the leaking loop was not assumed in this case because it would result in a transient similar to Case 1 or Case 3.

The discharge velocity of the fuel salt is evaluated based on the driving force as explained above. The simulation model is expressed as follows:

$$V_e(t) = \sqrt{2\{(P_{in}(t) - P_{out})/D_f + g(H_f^0 - H_b(t))\}} \quad (1)$$

$$P_{in}(t) = \frac{P_{in}(0) \cdot V_H^0}{V_H^0 + S \int_0^t V_e(t) dt} \quad (2)$$

$$H_b(t) = \frac{S \int_0^t V_e(t) dt}{A_{core}}, \quad (3)$$

where $P_{in}(t), P_{out}$: Reactor pressure and the external pressure (atmospheric)
 V_e : Discharge speed of fuel salt
 D_f : Fuel salt density
 g : Gravity
 V_H^0 : Initial volume of helium
 S : Break size
 H_f^0 : Initial fuel height (400 cm)
 $H_b(t)$: Reduction of fuel height
 A_{core} : Fuel flow area in the reactor; =(Fuel Salt Volume in the reactor)/ H_f^0

with the initial conditions of $P_{in}(0)=0.46$ MPa and $P_{out}=0.1013$ MPa.

For helium, the back pressure of 0.1 MPa is low enough to cause critical flow with the inner pressure of 0.46 MPa. However, as will be seen later, the inner pressure drops in quite a short time, so we neglected this effect. For fuel salt, such concern is not necessary because it is an incompressible fluid.

In order to know the sensitivity of the break size, we analyzed several cases with various effective break sizes. Although the effective break sizes are arbitrary, this sensitivity analysis provides the dependency of the pressure transient on the break size. Typical results are shown in **Fig. 6** for effective break sizes of 50 cm² and 100 cm². The reactor pressure drops quite rapidly to atmospheric pressure and then decreases gradually due to the leakage of the fuel salt by gravity. As can be expected, the larger the break size, the faster the pressure drop. The inner pressure drops to about 0.01 MPa. However the vapor pressure of the fuel salt is only 13.3 Pa or 0.1 mHg at a temperature of 894 K. Therefore no boiling of the fuel salt occurs. However in Case 2, bubble separation could be expected because the movements of the fuel salt and the bubbles are in opposite directions. The bubble separation causes a loss of voids, which results in a negative reactivity insertion. Also, the fuel volume in the reactor decreases and the neutron leakage increases. Based on these considerations, the bubble separation process

is modeled as follows.

Since the bubble diameter is so small, that the bubbles would soon reach their final velocity. The relative velocity of the bubbles to the fuel salt is evaluated based on the following equation

$$\frac{C_D^B}{2} \rho_L U_B^2 A_{Bubble} = \frac{\pi}{6} D^3 (\rho_L - \rho_V) g \quad (4)$$

$$C_D^B = \frac{18.5}{Re^{3/5}} \quad (5)$$

$$Re = \frac{U_B D}{\nu_L}, \quad (6)$$

where C_D^B : Drag coefficient of bubble
 ρ_L, ρ_V : Densities of fuel salt and helium, respectively
 U_B : Relative speed of bubble
 $A_{Bubble} = \frac{\pi D^2}{4}$: Cross section of a bubble
 D : Bubble diameter
 ν_L : Viscosity of fuel salt, μ/ρ_L .

Substituting Eqs. (5) and (6) into Eq. (4), and based on $\rho_V \ll \rho_L$, we obtain

$$U_B = \left(\frac{4}{55.5} g \frac{D^{1.6}}{\nu_L^{0.6}} \right)^{1/4}, \quad (7)$$

with

$$\nu_L = \frac{\mu_L}{\rho_L} = \frac{0.1 \text{ g}\cdot\text{s}^{-1}\cdot\text{cm}^{-1}}{3.33 \text{ g}\cdot\text{cm}^{-3}} = 0.03 \text{ cm}^2\cdot\text{s}^{-1}. \quad (8)$$

Bubbles move upward with the speed that is dependent on the inner pressure and exit the fuel salt. A pure fuel region is formed and extends from the bottom of the reactor to the surface of the fuel salt. The volume of the fuel without bubbles can be calculated as follows:

$$V_{Fuel}(t) = A_{core} \int_0^t U_B(t) dt, \quad (9)$$

$U_B(t)$ is evaluated as described above based on the pressure dependent bubble diameter, which is calculated from the bubble volume, which is inversely proportional to the pressure.

The elimination of voids results in negative reactivity, which corresponds to the product of the initial void fraction and the void reactivity coefficient. Thus the core average reactivity change due to the bubble separation is calculated as follows, assuming that the axial neutron flux distribution is flat:

$$\begin{aligned} \rho_{Bubble \text{ Separation}}(t) &= \alpha_V \{(Vf(t) - Vf_{ini})(V_{core} - V_{Fuel}(t)) \\ &\quad - Vf_{ini} V_{Fuel}(t)\} / V_{core} \\ &= \alpha_V \{Vf(t)(V_{core} - V_{Fuel}(t)) - Vf_{ini} V_{core}\} / V_{core}, \quad (10) \end{aligned}$$

where α_V : Void coefficient
 $Vf(t)$: Volume fraction of bubbles, which is inversely proportional to the pressure
 Vf_{ini} : Initial volume fraction of bubbles
 V_{core} : Total volume of fuel salt in the core=Initial core volume - $V_{Fuel}(t)Vf(t)$.

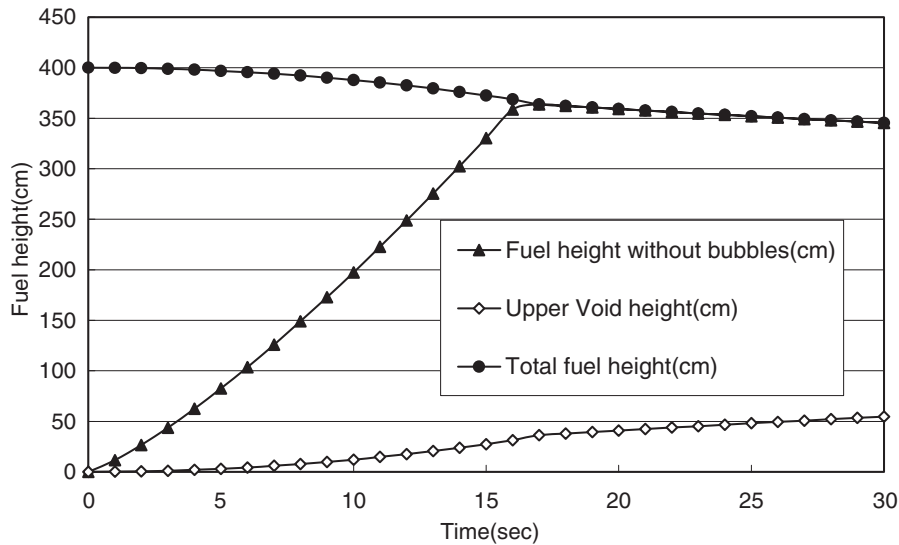


Fig. 7 Heights of each region in the core

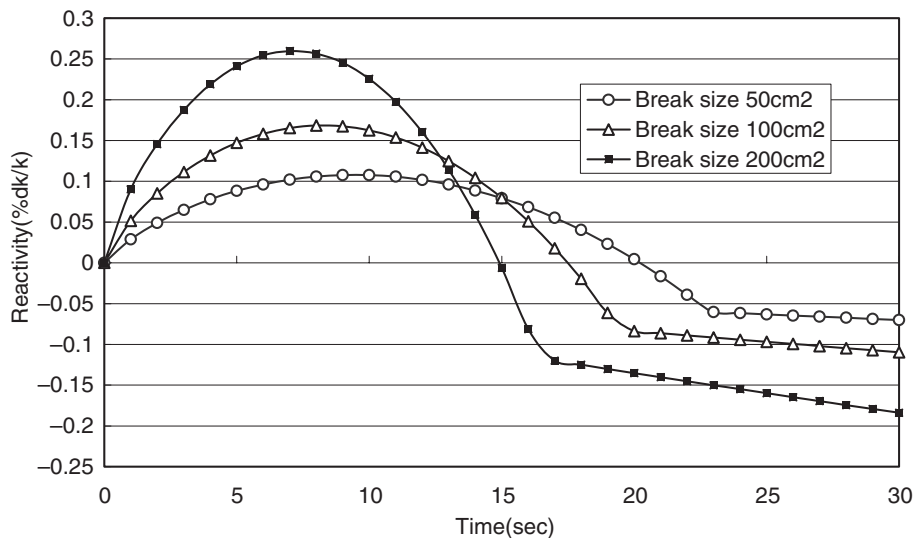


Fig. 8 Reactivity transient for the break near the reactor inlet

Moreover, the fuel height reduction due to the formation of a cavity at the top of the core also results in negative reactivity, which is evaluated as follows:

$$\rho_{\text{Height Reduction}}(t) = \frac{k_{\infty}}{1 + M^2 B_{RH}^2} - \frac{k_{\infty}}{1 + M^2 B_N^2}, \quad (11)$$

where M^2 : Migration area

B_{RH}^2 : Geometrical buckling with reduced core height

B_N^2 : Geometrical buckling with nominal condition.

Reduced core height can be calculated subtracting the cavity height from the initial fuel height. The cavity height is obtained by the product of the height of the region where bubbles have separated and the void fraction at the corresponding pressure. An example of the time dependent height of each region, that is, total fuel region, cavity region and the region without bubbles, is shown in Fig. 7. These are the results for a break size of 200 cm². The reactivity transient

evaluated by our procedure is shown in Fig. 8 for break sizes of 50, 100 and 200 cm². The last case is the most extreme case. This reactivity transient was passed to the simulator. As can be seen, the helium void is formed at the top of the core and the fuel flow stops in a short time. Thus, the fuel flow rate was assumed to be lost at the initiation of the break. The transient relative power and temperatures corresponding to a break size of 200 cm² is shown in Figs. 9 and 10, respectively. The maximum fuel outlet temperature was below 1,160 K for this extreme case. This break size is equivalent to a pipe diameter of about 16 cm, which would be a reasonable size for a two loop MSR with a rated power of 350 MWt.

5. Evaluation Model for the Depressurization Transient for Case 3

In this case the driving force for the fuel salt is provided

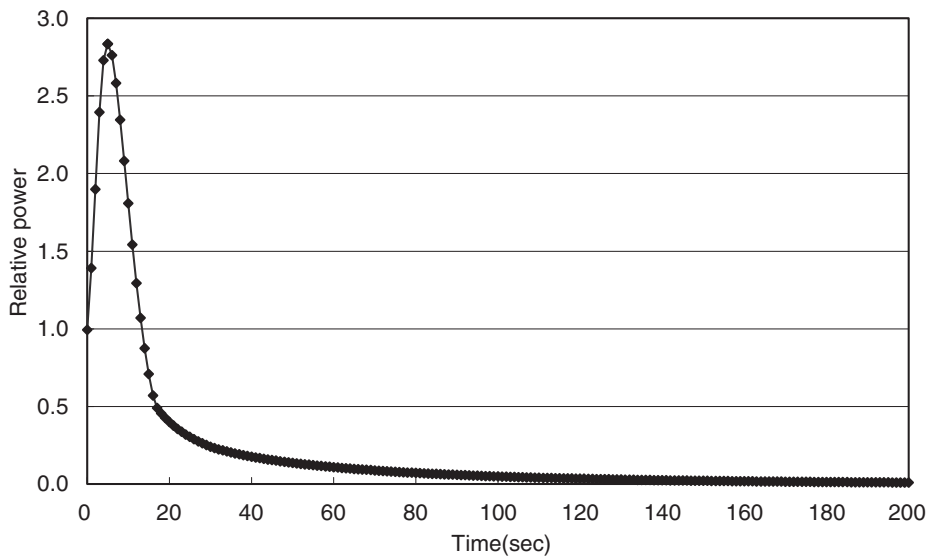


Fig. 9 Reactor transient with bubble separation and no fuel flow: Relative power

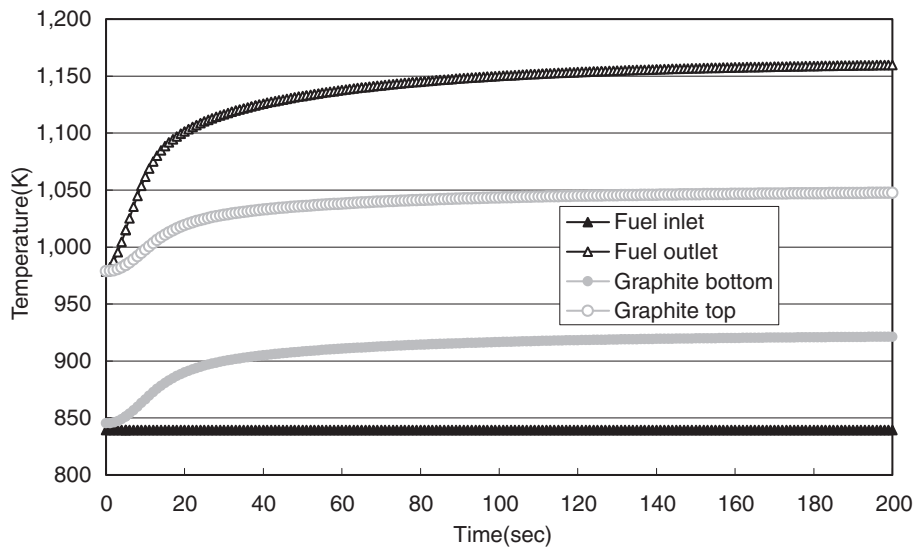


Fig. 10 Reactor transient with bubble separation and no fuel flow: Temperatures

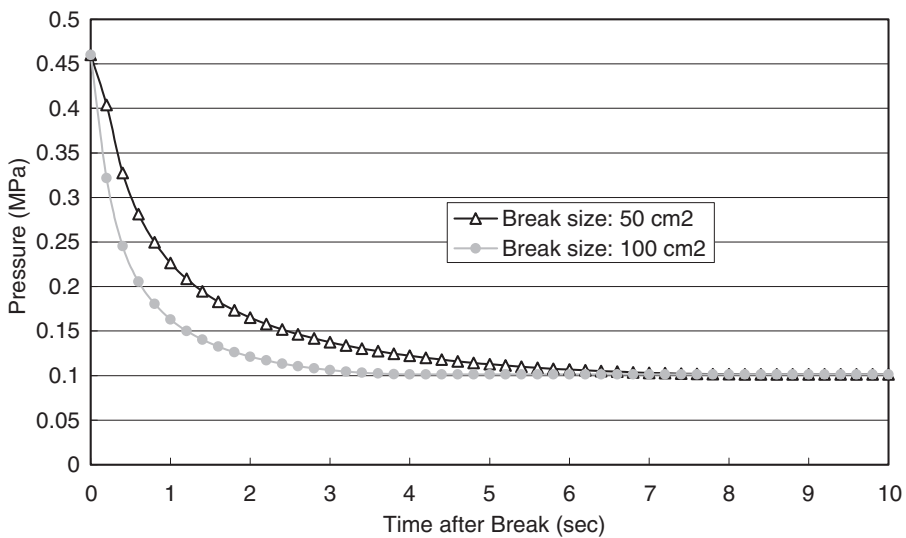


Fig. 11 Reactor pressure transient for the break at the exit of the reactor

only by the pressure difference between inner and outer pressures. Thus Eq. (1) is becomes

$$V_e(t) = \sqrt{2(P_{in}(t) - P_{out})/D_f}. \quad (12)$$

As explained above, an example of the analyses for the effective break sizes of 50 cm² and 100 cm² are shown in **Fig. 11**. The pressure drops within a few seconds. In this case the fuel salt flow could be maintained, however the loop that experienced the break was assumed to be isolated.

In addition, we accounted for the following phenomena. The bubbles and the fuel salt flow upward as the bubbles expand. The increased buoyancy of the bubbles accelerate the fuel salt flow. This acceleration effect was evaluated as follows in accordance with the previous discussion.

Using Eq. (7), the relative bubble velocity is about 12.5 cm/s for $D=0.05\sqrt[3]{5}=0.0855$ cm (5 times the volume after expansion).

The drag force is balanced by the drag force of the flow channel in order to establish the final velocity with the increased fuel flow speed.

Thus the equation is expressed as follows. Before the accident,

$$2\pi RL \frac{1}{2} \rho_L U^2 C_D^W = \pi R^2 \Delta P. \quad (13)$$

When the bubble expands,

$$2\pi RL \frac{1}{2} \rho_L (U + \Delta U)^2 C_D^W = \pi R^2 \Delta P + \frac{1}{2} C_D^B \rho_L U_B^2 \frac{\pi D^2}{4} N, \quad (14)$$

where R : Radius of the flow channel

L : Core height

$U, \Delta U$: Nominal fuel speed and the increased speed, respectively

C_D^W : Drag coefficient of the channel

ΔP : Pressure loss at normal operation

N : Number of bubbles in the channel, $\pi R^2 L \times 0.01 / (\pi D^3 / 6)$

(Volume fraction of 1% for helium bubbles)

U_B : Relative final speed of bubble, 12.5 cm/s

Re_L : Reynolds Number of fuel salt, $=2RV/\nu_L$

Re_B : Reynolds Number of bubble, $=DV/\nu_L$.

The increment of driving force due to the upward flow of the bubbles can be evaluated from the increment of the equivalent pressure in Eq. (13) as ΔP_B

$$\begin{aligned} \pi R^2 \Delta P_B &= \frac{1}{2} C_D^B \rho_L U_B^2 \frac{\pi D^2}{4} N, \text{ thus} \\ \Delta P_B &= \frac{1}{2} \cdot \frac{18.5}{Re_B^{0.6}} \rho_L U_B^2 \frac{\pi D^2}{4} \cdot \frac{L \times 0.01}{\frac{\pi D^3}{6}} \\ &= 0.13875 \left(\frac{\nu_L}{DU_B} \right)^{0.6} \rho_L U_B^2 \frac{L}{D} \\ &= 0.13875 \frac{LU_B^{1.4} \nu_L^{0.6} \rho_L}{D^{1.6}}. \end{aligned} \quad (15)$$

The increment of the driving force is about 40.4 gf/cm².

On the other hand, the normal pressure is 19 psi=19×(453/2.54²)=1,334 gf/cm². Thus

$$\left(\frac{U + \Delta U}{U} \right)^2 = \frac{1,334 + 40.4}{1,334} = 1.03. \quad (16)$$

Therefore,

$$\frac{U + \Delta U}{U} = 1.015. \quad (17)$$

It means that the acceleration is quite small. However when the mass flow rate is constant, the fuel velocity increases due to the expansion of bubbles, which is about 1%. Thus the total velocity increase is only about 2.5% and this effect is neglected in the present study.

We assume that the pressure drops within a step to atmospheric pressure as an extreme case. The initial pressure of 0.46 MPa drops to 0.1 MPa of atmosphere pressure when the accident occurs. Thus the void fraction will expand at most by a factor of 4.6. For a conservative evaluation, it was assumed that the initial void fraction of 0.2% expanded by a factor of 5. In other words, the void fraction was increased from 0.2 to 1.0% for a conservative analysis. Based on these assumptions and the void reactivity coefficient, the added reactivity is 0.08% $\Delta k/k$. Moreover, when the fuel salt temperature increases, the voids expand further with a corresponding increase in reactivity. We evaluated the maximum feedback effect on the reactivity as follows.

Assuming a constant system pressure, the void volume is obtained as,

$$\frac{P_D V_D}{T_D} = \frac{P V}{T}, \quad (18)$$

thus,

$$V = \frac{T}{T_D} V_D. \quad (19)$$

Since the definition of the void reactivity coefficient is

$$\alpha_V = \frac{\partial \rho}{\partial V} \quad (20)$$

and assuming that α_V is constant, the reactivity insertion due to the temperature rise is

$$\Delta \rho = \alpha_V \Delta V = \alpha_V (V - V_D) = \alpha_V \frac{T - T_D}{T_D} V_D, \quad (21)$$

where the subscript D denotes immediately after the accident. This estimation is conservative because a simultaneous temperature rise is assumed. When the temperature rise of the core is, say from 900 to 1,100 K, the void reactivity increase is about 0.02% $\Delta k/k$. Thus we analyzed the transient by using a step reactivity insertion of 0.11% $\Delta k/k$ instead of 0.10% $\Delta k/k$ obtained as the sum of the reactivity insertion above plus the temperature effect. The result is shown in **Figs. 12** and **13** for the relative power and the fuel salt and graphite temperatures, respectively. It is seen that the relative power jumped to about two times the rated power in a short time interval and then stabilized at 50% of the rated power level. The maximum fuel

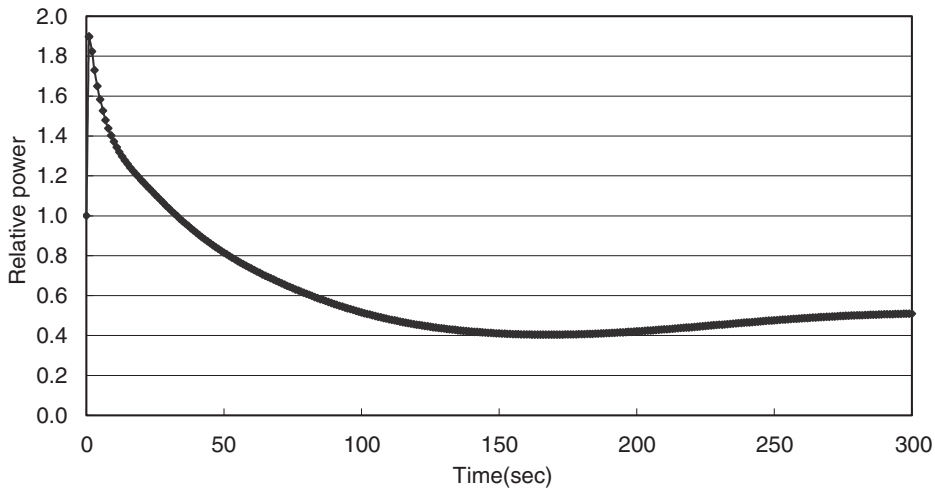


Fig. 12 Reactor transient after 0.11% $\Delta k/k$ step reactivity addition with 50% fuel flow: Relative power

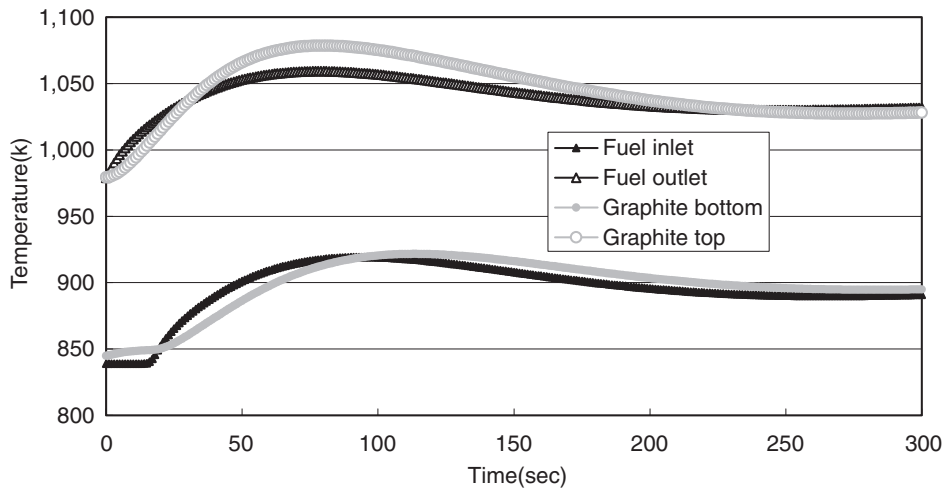


Fig. 13 Reactor transient after 0.11% $\Delta k/k$ step reactivity addition with 50% fuel flow: Temperatures

inlet and outlet temperatures are 920 K and 1,060 K, respectively.

V. Discussions

1. Safety Criteria for the MSR

For MSRs, no explicit safety criteria have yet been established. In this study we selected criteria based on the mechanical integrity of Hastelloy-N in order to avoid creep deformation based on the data of the Larson-Miller plot for Hastelloy-N.⁷⁾ The stress intensity for the evaluation is assumed to be those for the MSBR.

A preliminary elastic stress analysis for the reactor vessel of the MSBR was performed by ORNL.¹⁾ The analysis was based on the upper plenum of the vessel operating at 980 K and 0.39 MPa and the lower plenum at 866 K and 0.52 MPa. The maximum stress in the removable head due to pressure alone was 36.0 MPa. This stress was located in the reactor vessel head near the junction of the vessel head and shell. The maximum stress in the vessel occurred at

the junction of the lower head and shell and was 123 MPa.

As the fuel salt temperature could rise into the creep range, the allowable temperature must be determined by both stress and the duration in which the stress is loaded. We conservatively chose the maximum duration to be 1 h, which is long enough to shut down the reactor and take corrective actions. The maximum stress for both the top head and reactor vessel are assumed to be 43.4 MPa and 138 MPa, respectively, with a calculational uncertainty of 20%. Finally, the allowable deformation is chosen to be 1%. Assuming the temperature of Hastelloy-N is equal to that of the fuel salt, the allowable inlet and outlet temperatures are determined to be 1,060 K and 1,200 K, respectively.

2. Items to be Studied in the Future

As can be seen above, the estimation model of transient behaviors of the molten salt leakage is somewhat crude. In the analyses, we have simplified the actual phenomena for the ease of modeling. Thus in the future the validity of such assumptions need to be verified. They are as follows.

(1) More Precise Modeling of the Primary Loop for Transient Behavior during the Depressurization Accident

We assumed that a break between the fuel salt pump exit and the heat exchanger or a break at the exit of the reactor could result in isolation of the loop. However, transient behavior of the loss of flow should be analyzed in detail by simulation or experiment based on the actual system design data.

(2) Bubble Separation Behavior

We assumed that the bubbles in the fuel salt would separate when the fuel salt flowed downward. But how effectively this separation would occur should be verified by experiment.

(3) Bubble Merging during Expansion

We assumed that the expanding bubbles did not merge. But if some bubbles would merge then the bubble sizes would become larger and the final velocity would increase. The acceleration would also increase. The bubble density after the expansion would be about 3 to 4 bubbles per cubic centimeter. Although the bubble size is so small, less than 1 mm in diameter, the collision of bubbles would be limited. However some verification would be required.

(4) Critical Flow Phenomena during the Discharge of the Helium Mixed Flow

We have neglected the effect of the critical flow of helium because of the short interval of the phenomena. It is expected that inclusion of the effect would not be so large. However, this also should be verified by experiment.

(5) Other Accident Transients

Other accident transients should also be analyzed to thoroughly evaluate MSR safety. The results will be reported at some future time.

VI. Conclusion

We have analyzed a depressurization accident without scram in the Molten Salt Reactor, Fuji-12. The maximum inlet fuel temperature was 920 K in the event of a break at the outlet of the core. The maximum outlet temperature was 1,160 K in the event of a break near the inlet of the core. Based on preliminary temperature criteria, the inlet temper-

ature limit is 1,060 K and the outlet temperature limit is 1,200 K. Thus the depressurization accident without scram can be stabilized within the safety limit.

Although the maximum fuel temperature safety criteria were not violated, the calculated maximum outlet fuel temperature approached the limiting temperature of 1,200 K. This is due to the loss of total fuel flow. In MSRs, loss of fuel salt flow results in the loss of the heat sink. Thus it can be said that some mitigation system might be installed to protect against the loss of fuel salt flow. One such system is the salt drain which has been designed for the Molten Salt Breeder Reactor.

The above conclusions are based on the assumption that some essential design parameters such as helium void fraction and system pressure are identical to those of the MSBR. However for Fuji-12 the reactor power density is about 3 times lower than that of the MSBR. Thus the relevant parameters might be much milder and the transient behaviors could be less severe.

References

- 1) R. C. Robertson, *et al.*, *Conceptual Design Study of a Single-Fluid Molten-Salt Breeder Reactor*, ORNL-4541, Oak Ridge National Laboratory, Oak Ridge, TN, (1971).
- 2) K. Mitachi, T. Suzuki, Y. Nakanishi, D. Okabayashi, *et al.*, "A preliminary design study of a Small Molten Salt Reactor for effective use of thorium resource," *7th Int. Conf. on Nuclear Engineering*, Tokyo, Japan, 7144 (1999).
- 3) K. Mitachi, T. Suzuki, Y. Nakanishi, D. Okabayashi, R. Yoshioka, "Re-estimation of nuclear characteristics of a Small Molten Salt Power Reactor," *Nihon-Genshiryoku-Gakkai Shi (J. At. Energy Soc. Jpn.)*, **42**[9], 99 (2000), [in Japanese].
- 4) R. Yoshioka, Private communication.
- 5) Y. A. Chao, P. Huang, "Theory and performance of the Fast-Running Multidimensional Pressurized Water Reactor Kinetics Code, SPNOVA-K," *Nucl. Sci. Eng.*, **103**, 415 (1989).
- 6) K. Okumura, K. Kaneko, K. Tsuchihashi, *SRAC95; General Purpose Neutronic Code System*, JAERI-Data/Code 96-015, (1996), [In Japanese].
- 7) <http://www.haynesintl.com>, Haynes International, Inc.